Talanta 147 (2016) 177–183

Contents lists available at ScienceDirect

Talanta

journal homepage: www.elsevier.com/locate/talanta

Chemiluminescent aptasensor capable of rapidly quantifying *Escherichia Coli O157:H7*

Juna Khang [1], Danial Kim [1], Kang Wook Chung [1], Ji Hoon Lee *

Luminescent MD, LLC, Hagerstown, MD 21742, United States

ARTICLE INFO

Article history:
Received 24 August 2015
Received in revised form
21 September 2015
Accepted 22 September 2015
Available online 25 September 2015

Keywords:
Aptasensor
Food-borne pathogen
E. Coli O157:H7
Guanine chemiluminescence
Aptamer
Nanocomposites

ABSTRACT

Cost-effective and easy-to-use biosensor was developed for the rapid quantification and monitoring of *Escherichia* (*E.*) *Coli O157:H7* in sample using *E. Coli O157:H7* aptamer, graphene oxide (GO)/iron nanocomposites, and guanine chemiluminescence detection. *E. Coli O157:H7* aptamer-conjugated 6-carboxyfluorescein (6-FAM) with excellent specificity captured *E. Coli O157:H7* in a sample when the mixture was incubated for 1 h at 37 °C. Free *E. Coli O157:H7* aptamers remaining in sample after the incubation were removed with GO/iron nanocomposites based on the principle of π–π stacking interaction between free aptamer and GO/iron nanocomposites. Then, *E. Coli O157:H7* bound with aptamer-conjugated 6-FAM in sample emitted strong light when guanine chemiluminescent reagents (e.g., 3,4,5-trimethoxylphenylglyoxal hydrate, Tetra-*n*-propylammonium hydroxide) were added in the sample. The strength of light emitted in guanine chemiluminescence reaction was proportionally enhanced with the increase of *E. Coli O157:H7* concentration. The limit of detection (LOD) of biosensor capable of quantifying *E. Coli O157:H7* with good accuracy, precision, and reproducibility was as low as 4.5×10^3 cfu/ml. We expect that the rapid analytical system can be applied in the field of food safety as well as public health.

1. Introduction

Outbreak of foodborne pathogens with rapid globalization of food market in the last few decades is one of the critical problems in public health as well as food safety. For example, the Center for Disease Control and Prevention (CDC) recently reported that the number of foodborne diseases occurring in the United States are approximately 48 million cases per year (http://www.cdc.gov/foodborneburden/index.html). *Salmonella enterica, Staphylococcus aureus, pathogenic Escherichia coli, Listeria monocytogenes, Clostridium spp., Shigella spp*. and *Yersinia spp*. are the main foodborne pathogens causing the outbreak of infectious disease. Recently, for example, pathogenic *E. Coli* species such as *Escherichia* (*E.*) *coli O157:H7* accounted for a great majority of hospitalizations and deaths (http://www.cdc.gov/ecoli/).

In order to monitor and respond rapidly to outbreaks of foodborne pathogens, various analytical methods have been developed [1]. Unfortunately, most of methods and devices (e.g., culture-based horizontal method for detection and enumeration, molecular methods using real-time polymerase chain reaction (PCR), enzyme-linked immunosorbent assay (ELISA), electrochemical detection) require time-consuming culturing procedures of the samples, so they cannot rapidly sense and quantify foodborne pathogens [1]. Thus, only a very limited amount of the enormous domestic and imported foods that are released in the food market are being inspected using the conventional analytical system [2]. Recently, various aptamers using single strand DNA or RNA have been developed to capture foodborne pathogens in a sample [3–7]. Also, new analytical methods capable of rapidly quantifying trace levels of foodborne pathogens using aptasensors with chemiluminescence [8], colorimeter [7,9], electrochemical [9], or fluorescence [10] detection have been reported. Using aptasensors, it was possible to detect foodborne pathogens without complicated and tedious procedures such as multiple incubations and washings [8]. For example, Kwun and his collaborators reported that highly sensitive aptasensor with 1,1′-oxalyldiimidazole chemiluminescence detection can quantify *Vibrio parahaemolyticus* without time-consuming procedures such as multiple long-incubations and tedious washings [8].

Guanine, one of the four components – Adenine, Cytosine, Guanine, Thymine – of DNA aptamer, when reacting with 3,4,5-trimethoxylphenylglyoxal hydrate (TMPG), can produce a high-energy intermediate capable of emitting light by itself or transferring energy to fluorescent dye-conjugated with DNA aptamer based on the principle of intra chemiluminescence resonance energy transfer (Intra-CRET) as shown in Scheme 1 [11–13]. Light emitted from the reaction of DNA aptamer and TMPG in the

* Corresponding author. Fax: +1 301 393 9092.
E-mail address: jhlee@luminescentmd.com (J.H. Lee).
[1] Juna Khang, Danial Kim, Kang and Wook Chung contributed equally in this research.

http://dx.doi.org/10.1016/j.talanta.2015.09.055
0039-9140/

presence of tetra-*n*-propylammonium hydroxide (TPA) and N,N-dimethylformamide (DMF) is called guanine chemiluminescence [11]. Using two distinguishing characteristics (e.g., capture capable of rapidly binding with target material, CL reagent in guanine chemiluminescence reaction) of DNA aptamer, an aptasensor capable of rapidly sensing thrombin or prostate specific antigen (PSA) without time-consuming incubations and washings was developed [11,12].

DNA aptamer capable of rapidly binding *E. Coli O157:H7* in a sample with excellent specificity and selectivity contains multiple guanines [7]. Thus, it is possible to develop a novel analytical method capable of rapidly quantifying *E. Coli O157:H7* using *E. Coli O157:H7* aptamer-conjugated fluorescent dye and guanine chemiluminescence detection. The analytical method developed in experiments conducted based on the hypothesis is described in detail below.

2. Experimental

2.1. Chemical and materials

Multiple types of *E. Coli O157:H7* aptamer (EA) conjugated fluorescent dye, as shown below, were purchased from Alpha DNA (Montreal, Quebec, Canada).

1. **EA-1**: 5′-CCGGACGCTTATGCCTTGCCATCTACAGAGCAGGTGTGACGG-florescein-3′
2. **EA-2**: 5′-CCGGACGCTTATGCCTTGCCATCTACAGAGCAGGTGTGACGG-6-carboxyfluorescein (6-FAM)-3′
3. **EA-3**: 5′-CCGGACGCTTATGCCTTGCCATCTACAGAGCAGGTGTGACGG-Pacific Blue-3′
4. **EA-4**: 5′-CCGGACGCTTATGCCTTGCCATCTACAGAGCAGGTGTGACGG-Cy 3-3′

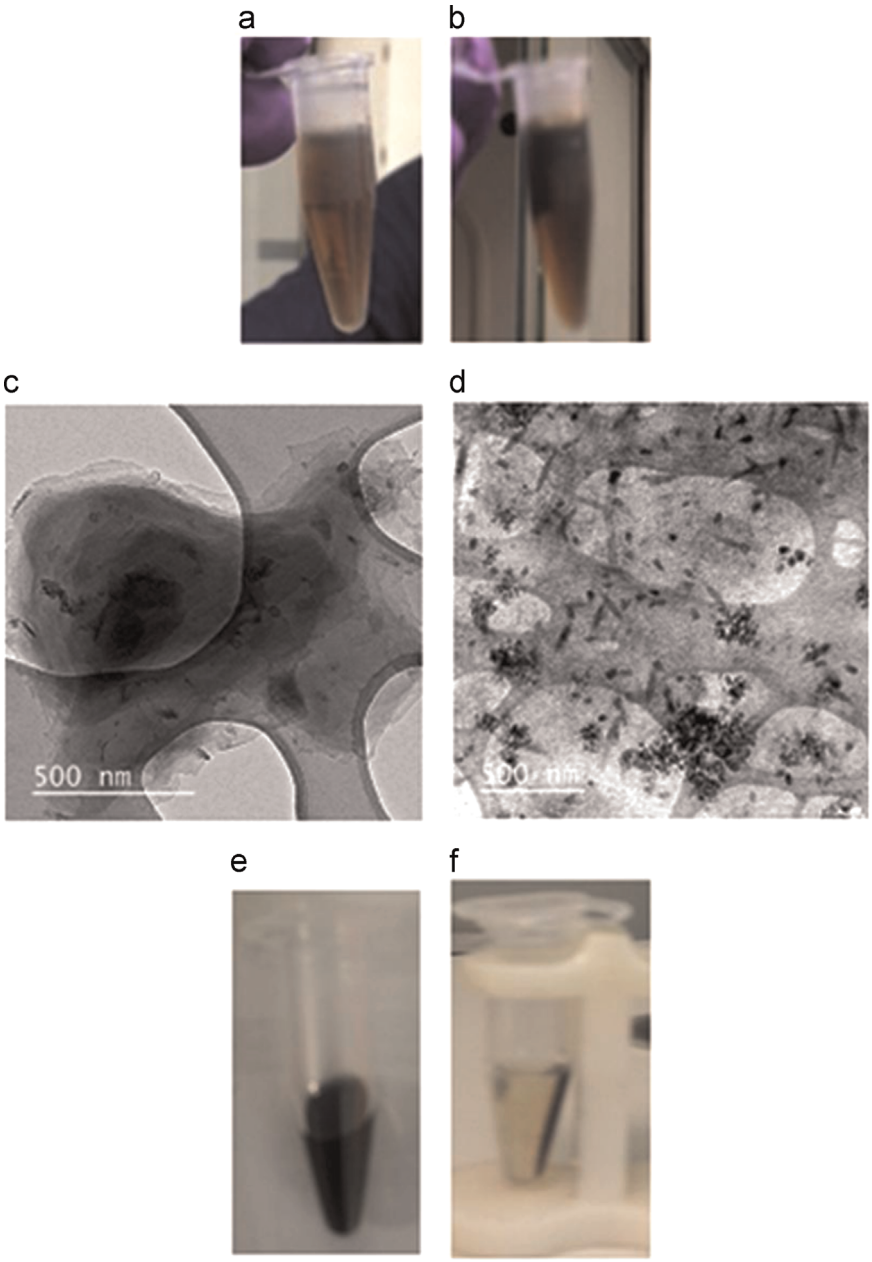

Fig. 1. Synthesis of GO/iron nanocomposite material. A: Mixture of GO, $FeCl_2$ and $FeCl_3$ in H_2O, B: GO/iron nanocomposite material (Fe_3O_4 GO) immediately formed with the addition of NH_4OH, C: GO taken using TEM, D: GO/Fe_3O_4 nanocomposite material taken using TEM, E: GO/iron nanocomposite material, F: Separation of GO/iron nanocomposite material using magnetic bar.

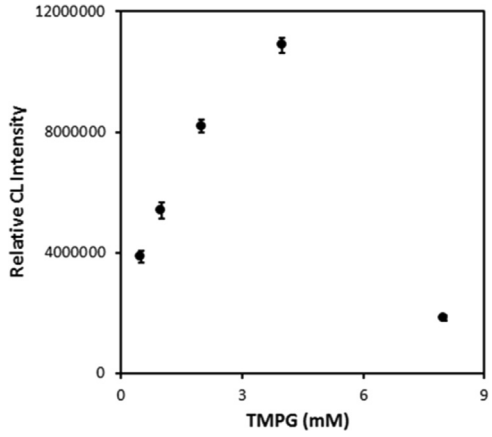

Fig. 2. Effect of TMPG concentration in guanine chemiluminescence reaction.

5. **EA-5**: 5′-6-FAM-CCGGACGCTTATGCCTTGCCATCTACAGAGCA-GGTGTG ACGG-3′
6. **EA-6**: 5′-6-FAM-GGGGGGTTTTCCGGACGCTTATGCCTTGCCATC-TACAGAGCAGGTGTG ACGG-3′

Pre-killed *E. Coli O157:H7* positive was purchased from KPL (Gaithersburg, MD, USA). 3,4,5-trimethoxylphenylglyoxal hydrate (TMPG, 97%) was purchased from Matrix Scientific (Columbia, SC, USA). $FeCl_2$ (99%), $FeCl_3$ (99%), Tetra-*n*-propylammonium hydroxide (TPA, 40% w/w aqueous solution), deionized H_2O (HPLC grade) were purchased from Alfa Aesar (Ward Hill, MA, USA). N,N-Dimethylformamide (DMF) and deionized water purchased from EMD (Billerica, MA, USA). Various types of buffer solutions (pH 7.0–8.5) were purchased from Teknova (Holliser, CA, USA). Graphene oxide (GO) was purchased from Graphene Supermarket (Calverton, NY, USA).

2.2. Fabrication of graphene oxide/iron nanocomposites

Graphene oxide/iron nanocomposites (Fe_3O_4 GO nanoparticles) were fabricated based on the previous report [7,14]. $FeCl_2$ (50 mg) and $FeCl_3$ (250 mg) were dissolved and mixed in water (20 ml). GO (1 mg/ml) was prepared in water. The mixture of $FeCl_2$ and $FeCl_3$ (0.5 ml) was mixed with GO (0.5 ml) in a 1.5 ml-centrifugetube as shown in Fig. 1(A). The tube inserted into a Micro Centrifuge Tube Thermo-mixer (Eppendorf) was shaken for 10 s at 85 °C. Then, ammonium hydroxide (NH_4OH, 20 μl, 30%) was dispensed into the tube as shown in Fig. 1(B). The microcentrifuge tube in the themomixer was shaken at 1000 rpm for 60 min at 85 °C. Fe_3O_4 GO nanoparticles formed in the microcentrifuge tube were cooled at room temperature (21 ± 2 °C). Fe_3O_4 GO nanoparticles in the microcentrifuge tube were washed 3 times in water using a magnetic separator (Bioclone,Inc.). Fe_3O_4 GO nanoparticles as a stock solution were stored in a refrigerator. As shown in Fig. 1(C) and (D), we obtained images of Fe_3O_4 GO nanoparticles with a Gatan Ultrascan 1000XP digital camera and a JEOL 2100 TEM operating at 200 kV accelerated voltage. Fig. 1(C) shows the shape of pure GO, whereas Fig. 1(D) indicates that the nanoparticles of Fe_3O_4 were anchored on the surface of GO. As shown in Fig. 1(E), free aptamer was immobilized on the surface of Fe_3O_4 GO nanoparticle based on the principle of π–π static interaction between free aptamer and Fe_3O_4 GO nanoparticles. Using the magnetic separator, free aptamers were immobilized on Fe_3O_4 GO nanoparticles were removed from the sample containing aptamer-bound *E. Coli O157:H7* as shown in Fig. 1(F).

2.3. Quantification of E. coli O157:H7 in sample

Several standards (e.g., 10^4, 10^5, 10^6, 10^7 cfu/ml) containing different concentration of *E. Coli O157:H7* and a sample containing a certain concentration of *E. Coli O157:H7* were prepared in PBS buffer. *E. Coli O157:H7* aptamer (100 nM, 100 μl), capable of capturing *E. Coli O157:H7* in sample was mixed with *E. Coli O157:H7* aptamer (100 μl). The mixture was incubated for 1 h at 37 °C. After the incubation, Fe_3O_4 GO nanoparticles (50 μl) in H_2O was added in the mixture. After 3-min of incubation, free aptamer immobilized on Fe_3O_4 GO nanoparticles was removed using the magnetic separator. The sample containing aptamer-bound *E. Coli O157:H7* (20 μl) was mixed with 20 mM TPA (10 μl) in a borosilicate test tube. Then, the test tube was inserted into the luminometer (Lumat LB 9507, Berthold, Inc., Germany). Finally, CL that was immediately emitted in the test tube after the addition of 4 mM TMPG (100 μl) through a syringe pump of luminomeer was measured for 20 s.

3. Results and discussion

3.1. Effect of TMPG concentration in quanine chemiluminescence

As shown in Fig. 2, the brightness of light emitted in guanine chemiluminescence was dependent on the concentration of TMPG. Relative CL intensity measured in the presence of 4 mM TMPG was the highest under this condition (2 μM aptamer-conjugated 6-FAM, 20 mM TPA). However, relative CL intensity measured with the addition of 8 mM TMPG sharply decreased due to self-quenching. In other words, excess high-energy intermediates formed under this condition was rapidly decomposed due to the collisional quenching before transferring energy to 6-FAM based on the principle of CRET shown in Scheme 1. In addition, the relative CL intensity in the presence of 5 mM TMPG was slightly lower than that in the presence of 4 mM TMPG. Also, the brightness of the light emitted in the presence of 6 mM was much weaker than that in the presence of 4 mM TMPG due to self-quenching even though the light of the former was brighter than that in the presence of 8 mM TMPG.

Based on the results shown in Fig. 2, 4 mM TMPG was selected in this research to develop highly sensitive analytical method for monitoring *E. Coli O157:H7* in a sample.

3.2. Effect of TPA concentration in guanine chemiluminescence

Fig. 3 shows that the strength of CL emission is dependent on the concentration of TPA used as a catalyst in guanine chemiluminescence reaction. Fig. 3 indicates that the appropriate concentration range of TPA to develop a biosensor, capable of rapidly

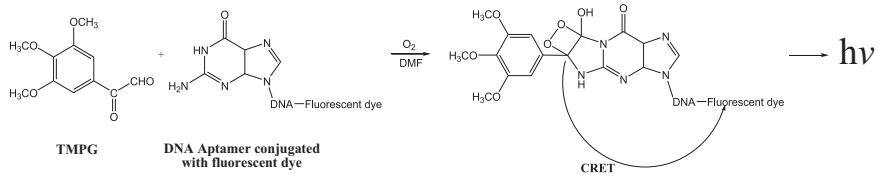

Scheme 1. Chemiluminescence resornance energy transfer (CRET) in guanine chemiluminescence reaciton.

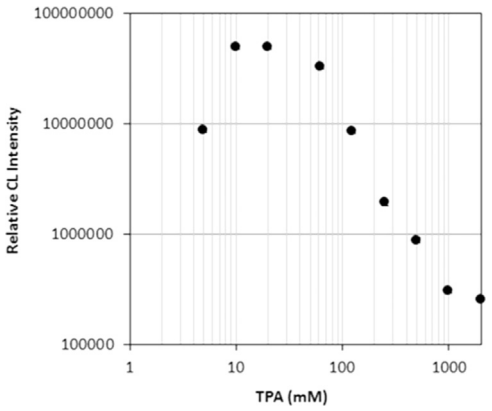

Fig. 3. Effect of TPA concentration in guanine chemiluminescence reaction.

quantifying trace levels of *E. Coli O157:H7*, under this condition (2 μM aptamer-conjugated 6-FAM and 4 mM TMPG) is 10–20 mM. Relative CL intensity measured in the presence of higher concentration of 20 mM TPA was exponentially decreased.

The pH of 20 mM TPA solution was 12.3 which was similar to that of 10 mM TPA solution (pH 12.1). With the increase of TPA concentration, however, the pH of the solution was shifted to a more basic condition. For example, the solution containing a higher concentration of 1 M TPA was too basic to measure the pH (> 14.0). Also, the pH of solution containing 5 mM TPA was less than 12. These results indicate that the appropriate pH in guanine chemiluminescence reaction in the presence of TPA is slightly higher than 12. Thus, the results shown in Fig. 3 is the proof that the brightness of guanine chemiluminescence depends on the pH because the light emitted in the presence of 10 or 20 mM TPA was brighter than those in the presence of lower than 10 mM TPA or higher than 20 mM TPA.

Based on the results shown in Fig. 3 we selected 20 mM TPA to develop a new analytical system for the quantification and monitoring of *E. Coli O157:H7* in a sample.

3.3. Effect of fluorescent dye in guanine chemiluminescence

As shown in Fig. 4, we confirmed that brightness of guanine chemiluminescence is dependent on the physical property of fluorescent dye emitted after receiving energy from high-energy intermediate formed in the reaction of guanine and TMPG in the presence of TPA. The relative CL intensity of aptamer-conjugated 6-FAM (e.g., EA-2, EA-5) was higher than those of other aptamer-conjugated fluorescent dyes such as fluorescein (EA-1), pacific blue (EA-3), and Cy 3 (EA-4). The results imply that the emission wavelength of high-energy intermediate formed from the reaction of TMPG and guanines of aptamer-conjugated 6-FAM is similar to the excited wavelength (492 nm) of 6-FAM in aqueous solution.

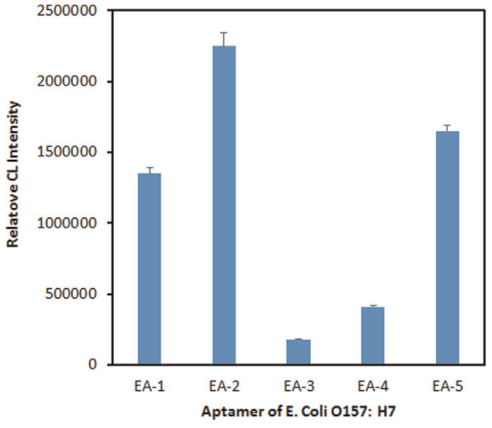

Fig. 4. Effect of fluorescent dye in CRET occurred in guanine chemiluminescence reaction.

In addition, Fig. 4 indicates that the strength of light emitted in guanine chemiluminescence reaction is dependent on the position of fluorescent dye labeled with aptamer. CL emission of 6-FAM conjugated with 3′-end of aptamer (EA-2) was brighter than that of 6-FAM conjugated with 5′-end of aptamer (EA-5). This is because 6-FAM of EA-2 (5′-CCGGACGCTTATGCCTTGCCATCTACAGAGCAGG TGTGAC**GG-6-FAM**-3′) was directly labeled with guanine positioned at 3′-end of aptamer, whereas 6-FAM of EA-5 (5′-**6-FAM-CC**GGACGCTTATGCCTTGCCATCTACAGAGCAGGTG TGACGG-3′) was connected with cytosine at 5′-end of aptamer. Thus, EA-2 can emit relatively strong light because 6-FAM can receive energy from high-energy intermediates, formed from the reaction of TMPG and guanines positioned at 3′-end of aptamer, without any interferences such as adenine, cytosine, and thymine. However, CL emission of EA-5 cannot be as strong as that of EA-2 because the two cytosines positioned between 6-FAM and guanine, as shown in the sequence of EA-5, inhibit intra-CRET between 6-FAM and high-energy intermediate formed from the reaction of guanine and TMPG.

3.4. Study of binding interaction between E. coli O157:H7 and aptamer

With the understanding of differences between EA-2 and EA-5 in guanine chemiluminescence reaction based on the results shown in Fig. 4, we modified EA-5 to enhance the strength of light emitted in guanine chemiluminescence reaction as EA-6 (5′-**6-FAM-GGGGGG**TTTT**CC**GGACGCTTATGCCTTGCCATCTACAG-AGCGGTGTGACGG-3′) based on research result reported by Cha and his collaborators [12]. 6-FAM conjugated with 5′ end of aptamer was directly connected 6 guanines without changing the sequence of *E. Coli O157:H7* aptamer. Also, 4 thymines were added in the modified aptamer as a linker to connect *E. Coli O157:H7* aptamer and 6 guanines. Thus, as shown in Fig. 5, relative CL intensity of EA-6, modified with EA-5, measured in the absence of *E. Coli O157:H7* was enhanced and was similar to that of EA-2.

As shown in Fig. 5, relative CL intensities of EA-2 and EA-6 in the presence of *E. Coli O157:H7* were higher than those in the absence of *E. Coli O157:H7*. These results indicate that EA-2 and EA-6 can capture *E. Coli O157:H7* in a sample. Also, Fig. 5 shows that light emitted from EA-2 or EA-6 bound with *E. Coli O157:H7* is stronger than that of free EA-2 or EA-6 as seen in the diagrams shown in Fig. 6. The result indicate that guanines, directly and consecutively connected with 6-FAM, of EA-2 or EA-6 bound with *E. Coli O157:H7* can react with TMPG to produce high-energy

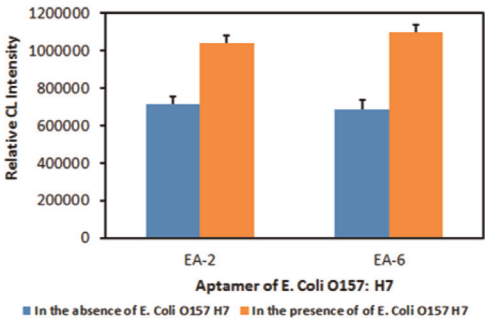

Fig. 5. Interaction between *E. Coli O157:H7* and aptamer of *E. Coli O157:H7*. Condition: [aptamer]=500 nM, [*E. Coli O157:H7*]=10^7 cfu/ml, [TMPG]=4 mM, [TPA]=20 mM.

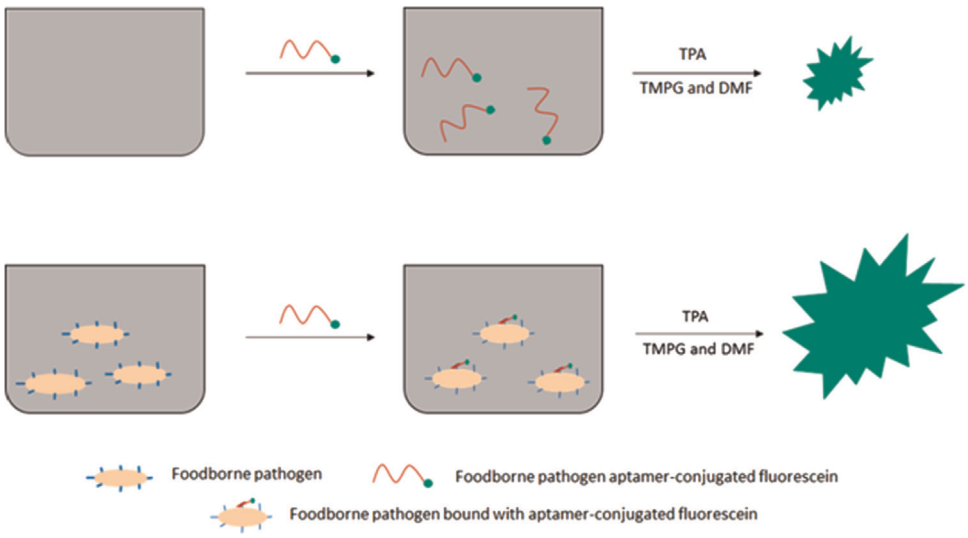

Fig. 6. CL emissions of free aptamer and aptamer bound with *E. coli O157:H7*.

intermediates. Then, 6-FAM can emit strong CL emission after the intra-CRET between high-energy intermediate and 6-FAM.

3.5. Effect of aptamer concentration

Based on the results shown in Fig. 6, we measured relative CL intensity in the absence and presence of *E. Coli O157:H7* with the addition of 5 different concentrations – 62.5, 125, 250, 500, 1000 nM – of aptamer. Then, we calculated the ratio in the presence of a certain concentration of aptamer as shown in Fig. 7. With the decrease of aptamer (EA-2 and EA-6) concentration, the ratio was increased. Thus, the ratio computed in the presence of 62.5 nM aptamer was the highest because the concentration of free aptamer remaining after the binding of aptamer and *E. Coli O157:H7* in the presence of 62.5 nM aptamer is lower than that in the presence of higher aptamer concentration than 62.5 nM. In other words, the concentration of aptamer used to bind with *E. Coli O157:H7* in the presence of 1000 nM aptamer is so low that relative CL intensity in the presence of *E. Coli O157:H7* was slightly higher than that in the absence of *E. Coli O157:H7*.

As shown in Fig. 7, the ratio in the presence of EA-6 is greater than that in the presence of EA-2. In particular, the ratio (12.5) in the prescience of 62.5 nM EA-6 was about 4.2-fold greater than that (2.95) in the presence of 62.5 nM EA-2. This is because additional 6 guanines of EA-6 modified to enhance CL emission of EA-5 can freely react with TMPG to produce high-energy intermediates while *E. Coli O157:H7* aptamer linked to 6 guanines are used to capture E. Coli O157:H7.

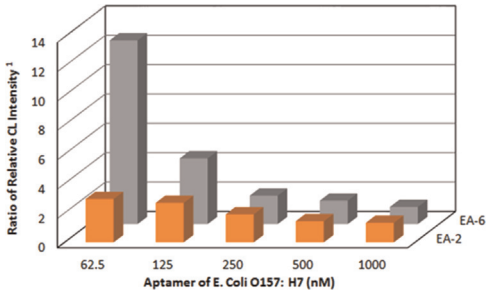

Fig. 7. Ratio of relative CL intensity in the absence and presence of *E. Coli O157:H7* with the addition of different concentration of aptamer of *E. Coli O157:H7*. Condition: [*E. Coli O157:H7*] = 10^7 cfu/ml, [TMPG] = 4 mM, [TPA] = 20 mM.

3.6. Removal of free aptamer after capturing E. coli O157:H7 in sample

Based on the experimental results shown in Fig. 7, it is possible to develop a new biosensor capable of rapidly quantifying *E. Coli O157:H7* in sample because relative CL intensity is proportionally enhanced with the increase of *E. Coli O157:H7*. However, it is difficult to develop highly sensitive biosensor because background measured from the biosensor without the removal of free aptamer is too high as shown in Fig. 8.

In order to reduce the background of biosensor, we synthesized GO/iron nanocompistes (Fe_3O_4 GO nanoparticles) as described in Section 2.2. As shown in Fig. 8, we were able to remove free aptamer remaining after the binding of aptamer and *E. Coli O157:H7* using GO/iron nanocomposites. This is because free aptamer, single strand DNA, is rapidly immobilized on the surface of GO/iron nanocomposites due to the π–π static interaction between two materials, whereas aptamer-bound *E. Coli O157:H7* does not interact with GO/iron nanocomposites.

3.7. Development of analytical system capable of rapidly quantifying E. Coli O157:H7 in a sample

Based on the results described above, we developed a biosensor for the quantification of *E. Coli O157:H7* in a sample. As shown in Figs. 6 and 8, *E. Coli O157:H7* aptamer (100 nM, EA-6) was added in the sample. Then, the mixture was incubated for 1 h at 37 °C. After the incubation, free aptamers remaining in sample were removed using GO/iron nanocomposites and magnetic bar. Finally, *E. Coli O157:H7* in the sample was quantified with the relative CL intensity emitted in the sample and the calibration curve shown in Fig. 9.

As shown in Fig. 9, sample containing lower *E. Coli O157:H7* than 10^4 cfu/ml was not quantified with the biosensor with guanine chemiluminescence even though relative CL intensity was slightly enhanced with the increase of *E. Coli O157:H7* concentration (see Fig. 9(A). Thus, it was possible to quantify higher *E. Coli O157:H7* than 10^4 cfu/ml because relative CL intensity was rapidly enhanced with the increase of *E. Coli O157:H7* concentration. As shown in Fig. 9(B), the dynamic range of linear calibration curve of biosensor was 10^4–10^7 cfu/ml. The limit of detection (LOD = background + 3 s) of biosensor was as low as 4.5×10^3 cfu/ml. LOD of cost-effective biosensor, capable of

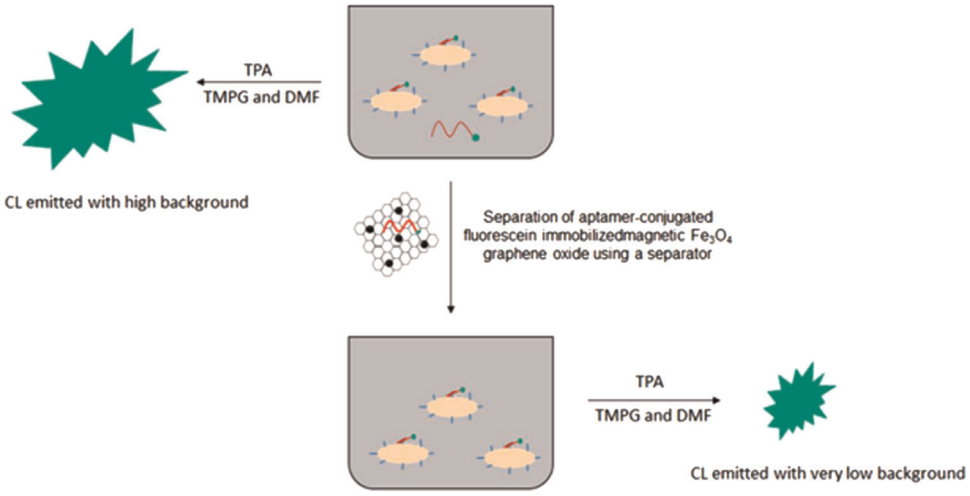

Fig. 8. Measurement of light emitted from aptamer bound with *E. Coli O157:H7* after separating free aptamer using Fe_3O_4 GO.

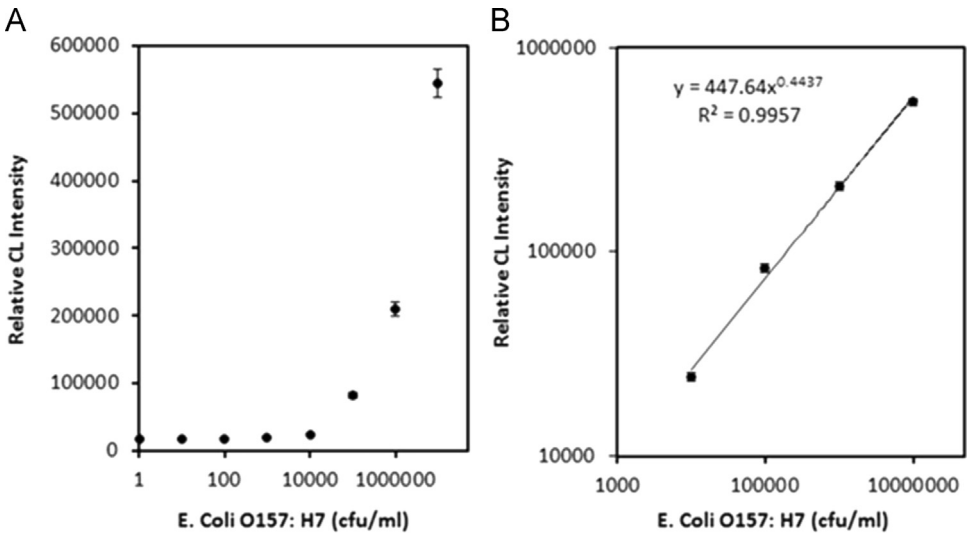

Fig. 9. Calibration curve for the quantification of *E. Coli O157:H7*.

Table 1
Recovery of biosensor for the quantification of *E. Coli O157:H7* ($N=5$).

Sample A[a]	Sample B[a]	Expected[a,b]	Measured[a]	Recovery (%)
10^5	2×10^4	6×10^4	$5.6\ (\pm0.2)\times10^4$	93.3
10^5	2×10^5	1.5×10^5	$1.42\ (\pm0.07)\times10^5$	94.7
10^5	2×10^6	5.5×10^5	$5.72\ (\pm0.14)\times10^5$	104

[a] Unit of *E. Coli O157:H7* concentration: cfu/ml.
[b] Expected value=(sample A+sample B)/2.

quantifying *E. Coli O157:H7* with 1 h and without time-consuming procedures such as multiple washings, was lower than those of conventional EIAs (1.0×10^5 cfu/ml) requiring expensive antibodies and enzyme, multiple-time incubations, and time-consuming washings [15].

Table 1 shows that the recovery of biosensor determined with the calibration curve of Fig. 9(B) is acceptable for the quantification of *E. Coli O157:H7* spiked in skim milks. Also, Table 1 indicates that accuracy and precision of biosensor are good within acceptable error range.

4. Conclusion

Using *E. Coli O157:H7* aptamer (EA-6) modified with EA-5, GO/iron nanocoposites, we developed an easy-to-use biosensor with guanine chemiluminescence detection for the rapid quantification and monitoring of *E. Coli O157:H7* in sample. The method was more cost-effective, faster, and simpler than conventional EIAs. Also, *E. Coli O157:H7* aptamer used to develop the biosensor was stable at ambient condition, whereas antibodies used in EIAs are expensive and intractable.

We expect that method developed in this research can be applied in quantifying other food-borne pathogens such as salmonella, listeria, and vibrio. As shown in Fig. 4, color of light emitted in guanine chemiluminescence reaction is determined by fluorescent dye labeled with aptamer. Thus, as future work, we will be able to develop an advanced biosensor capable of simultaneously quantifying and monitoring multiple types of food-borne pathogens in a sample.

Acknowledgment

This research was performed based on the intern program (LST-2014-5) of Luminescent MD, LLC.

References

[1] F. Yeni, S. Acar, O.G. Polat, Y. Soyer, H. Alpas, Rapid and standardized methods for detection of foodborne pathogens and mycotoxins on fresh produce, Food Control 40 (2014) 359–367.
[2] R.A. Holley, Food safety challenges within north american free trade agreement (NAFTA) partners, Compr. Rev. Food Sci. Food Saf. 10 (2011) 131–142.
[3] Y.J. Lee, S.R. Han, J.S. Maeng, Y.J. Cho, S.W. Lee, In vitro selection of *Escherichia coli* O157:H7-specific RNA, Biochem. Biophys. Res. Commun. 417 (2012) 414–420.
[4] J.A. DeGrasse, A single-stranded DNA aptamer that selectively binds to *Staphylococcus aureus* Enterotoxin B, Plos One 7 (2012) e33410.
[5] G.Q. Liu, X.F. Yu, F. Xue, W. Chen, Y.K. Ye, X.J. Yang, Y.Q. Lian, Y. Yan, K. Zong, Screening and preliminary application of a DNA aptamer for rapid detection of Salmonella O, Microchim. Acta 178 (2012) 237–244.
[6] H.P. Dwivedi, R.D. Smiley, L.A. Jaykus, Selection of DNA aptamers for capture and detection of Salmonella Typhimurium using a whole-cell SELEX approach in conjunction with cell sorting, Appl. Microbiol. Biotechnol. 97 (2013) 3677–3686.
[7] W.H. Wu, M. Li, Y. Wang, H.X. Ouyang, L. Wang, C.X. Li, Y.C. Cao, Q.H. Meng, J. X. Lu, Aptasensors for rapid detection of *Escherichia coli* O157:H7 and Salmonella typhimurium, Nanoscale Res. Lett. 7 (2012) 658.
[8] J. Kwun, S.Y. Yun, L. Park, J.H. Lee, Development of 1,1′-oxalyldiimidazole chemiluminescent biosensor using the combination of graphene oxide and hairpin aptamer and its application, Talanta 119 (2014) 262–267.
[9] N. Paniel, J. Baudart, Colorimetric and electrochemical genosensors for the detection of *Escherichia coli* DNA without amplification in seawater, Talanta 115 (2013) 133–142.
[10] J.S. Maeng, N. Kim, C.T. Kim, S.R. Han, Y.J. Lee, S.W. Lee, M.H. Lee, Y.J. Cho, Rapid detection of food pathogens using RNA aptamers-immobilized slide, J. Nanosci. Nanotechnol. 12 (2012) 5138–5142.
[11] S. Cho, L. Park, R. Chong, Y.T. Kim, J.H. Lee, Rapid and simple G-quadruplex DNA aptasensor with guanine chemiluminescence detection, Biosens. Bioelectron. 52 (2014) 310–316.
[12] T. Cha, S. Cho, Y.T. Kim, J.H. Lee, Rapid aptasensor capable of simply diagnosing prostate cancer, Biosens. Bioelectron. 62 (2014) 31–37.
[13] M. Yamasuji, T. Shibata, T. Kabashima, M. Kai, Chemiluminescence detection of telomere DNA in human cells on a membrane by using fluorescein-5-isothiocyanate-labeled primers, Anal. Biochem. 413 (2011) 50–54.
[14] H.K. Choi, J.H. Lee, Role of magnetic Fe_3O_4 graphene oxide in chemiluminescent aptasensors capable of sensing tumor markers in human serum, Anal. Methods 5 (2013) 6964–6968.
[15] Y. Zhang, C. Tan, R. Fei, X. Liu, Y. Zhou, J. Chen, H. Chen, R. Zhou, Y. Hu, Sensitive chemiluminescence immunoassay for *E. coli* O157:H7 detection with signal dual-amplification using glucose oxidase and laccase, Aanl. Chem 86 (2014) 1115–1122.